Tri-Band Endfire Antenna Array with Wide Angles of Beam-Scanning Capability for 5G mmWave Mobile Communication

Ali Zidour
Department of Electrical systems Engineering, Faculty of Technology University of M'hamed Bougara
Boumerdes, Algeria
a.zidour@univ-boumerdes.dz

Mouloud Ayad
Department of Electrical systems Faculty of Sciences and Applied Sciences University of Bouira
Bouira, Algeria
m.ayad@univ-bouira.dz

Mohammad Alibakhshikenari
Department of Signal Theory and Communications
Universidad Carlos III de Madrid Leganés
Madrid, Spain
mohammad.alibakhshikenari@uc3m.es

Haleh Jahanbakhsh Basherlou
School of Computing, Engineering and the Built Environment
Edinburgh Napier University
Edinburgh, UK
h.jahanbakhshBasherlou@napier.ac.uk

Naser Ojaroudi Parchin
School of Computing, Engineering and the Built Environment
Edinburgh Napier University
Edinburgh, UK
n.ojaroudiParchin@napier.ac.uk

Chan Hwang See
School of Computing, Engineering and the Built Environment
Edinburgh Napier University
Edinburgh, UK
c.see@napier.ac.uk

Abstract—In this paper, a novel multiband phased array antenna with endfire radiation pattern is designed at millimeter-wave (mmWave) frequency bands for 5G mobile applications. The proposed antenna element is a compact quasi-Yagi with a modified dipole driver to generate multiband operation, arranged on low-loss RO4003C materiel. The antenna array achieves excellent performance and covers wide frequency ranges of (24.15-29.8 GHz), (36.2-50 GHz) to support 5G NR bands; 26, 28, 39 and the new allocated 48 GHz. The array can exhibit a maximum realized gain from 8.4 dBi to 11.8 dBi. The radiated beam can be steered to cover wide scan angles by varying the phase shift and fulfilling beam-scanning applications.

Index Terms—5G NR, mmWave, endfire radiation, multiband antenna, beamforming, beam-scanning

I. INTRODUCTION

The ongoing fifth-generation of mobile communication (5G), featuring higher data rates of up to several Gbps, more reliable wireless links and ultra-low latency, uses mmWave bands that have been allocated to unleash the full potential of such promising cellular technology [1]–[3]. However, several challenges and issues for antenna designers are owing to the severe losses over wireless channels and the limited space allocated for antenna integration in the latest commercial handsets. Therefore, antenna arrays and beamforming techniques with high gain and beam steering ability are widely adopted in mmWave communication to compensate for the higher propagation losses and the shadowing effect in non-line of sight (NLOS) environment [4]–[6]. Besides, mm-wave arrays with end-fire radiation patterns are frequently preferred due to their edge-positioned merit and wide spatial coverage ability for practical applications [7], [8].

In recent years, several 5G mmWave antenna systems have been investigated with endfire radiation for mobile terminals, including quasi-Yagi antenna [9], [10], electric dipole antenna [11], Vivaldi antenna [12], and metasurface antenna [13]. Even though, the mentioned antennas featuring with good radiation performance at various mmWave frequencies, the majority have a limited operation bandwidth. Furthermore, recent design criteria have imposed very limited space in the mobile terminals to integrate mmWave antenna arrays since flagship handsets are excessively featured of full-screens and bigger batteries. Thereby, compact phased arrays are required.

TABLE I: 5G NR Operating Bands in FR2 [14]

Operating Band	Frequency Range
n257	26.50 GHz - 29.50 GHz
n258	24.25 GHz - 27.50 GHz
n259	39.50 GHz – 43.50 GHz
n260	37.00 GHz - 40.00 GHz
n261	27.50 GHz – 28.35 GHz
n262	47.20 GHz – 48.20 GHz

According to the latest 3GPP TS 38.101-2 release 17.4.0, 5G new radio (NR) spectrum allocations at frequency range 2 (FR2) are selected as listed in Table I [14]. Four bands around 26 GHz, 28 GHz, 39 GHz and 48 GHz, are basically of interest to antenna designers.

The investigation of beamforming antenna arrays with the multiband operation and endfire radiation is still an untapped topic. Several feasible solutions for wideband and multiband mmWave operation have also been discussed. Therefore, antenna array with independent radiation pattern characteristics

are proposed in [15] to achieve dual-band operation based on the integration of two antenna arrays which increases complexity and power consumption. Metasurface-based antenna are proposed in [16] for the dual-band operation in 5G mmWave systems using characteristic mode analysis to predict resonant modes and feed positioning. In [17], [18], dual-band antenna designs to cover 26 GHz or 28 GHz and 39 GHz bands using stacked capacitive fed resonant elements. Although some approaches have been employed to achieve multiband operation and enhance the bandwidth of each band, the operating bands are still unmatched with recent 5G NR bands at the cost of the bulky structure and broadside radiation pattern. Thus, novel multiband antenna arrays with endfire radiation patterns to cover the bands of interest are required to reduce complexity, power consumption, and keep the number of antennas under control. Such design criteria are very challenging, mainly owing to the difficulty of obtaining an adequate impedance bandwidth to cover the bands of interest.

A miniaturized multiband antenna array with larger scanning angles is presented in this paper, which could be installed into handheld smart devices wherein antenna resonators are arranged in a linear array form at the edge of the mainboard. All 5G NR bands can be supported by the proposed array with bandwidth extending from 24 to 29.8 GHz and from 36.2 to 50 GHz for -10 dB impedance bandwidth criterion.

II. Antenna Element Design
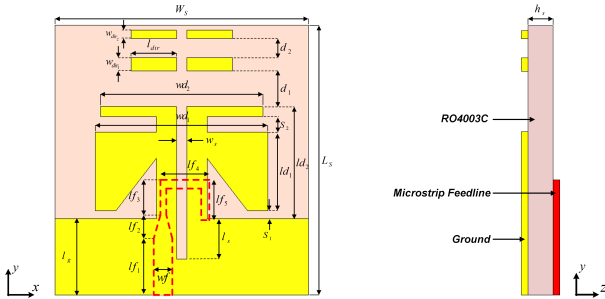
Fig. 1: Configuration and detailed dimensions of the antenna element.

As shown in Fig. 1, the configuration of the proposed antenna array element is printed on a 5 Mil Rogers RO4003C substrate layer (ϵ_r = 3.55, and tanδ = 0.0027). The quasi-Yagi antenna element consists of a bow tie dipole driver with two protruding strips coexisting at the same side of the truncated ground plane and two parasitic spaced strips as directors for effectively generating high gain endfire radiation pattern. On the opposite substrate side, a balun structure is used to feed the dipole through a slot line. which consists of a folded line connected to 50 Ω microstrip line. The impedance matching was achieved by adjusting the feeding point. In addition, dipole arms (wd_s) and the gap of the slot line (w_s) are critical design parameters. The values of design parameters are provided in Table II.

TABLE II: Design Parameter Values (Units in Millimeters)

Par.	L_s	W_s	l_g	ld_1	ld_2	wd_1	wd_2	s_1
Value	5.3	5	1.5	1.6	2	3.6	3.3	0.1
Par.	s_2	l_s	w_s	lf_1	lf_2	lf_3	lf_4	lf_5
Value	0.2	0.8	0.2	1.1	0.49	0.5	0.85	1
Par.	wf	wf_1	wf_2	$_ldir$	w_{dir_1}	w_{dir_2}	d_1	d_2
Value	0.37	0.15	0.2	0.95	0.2	0.15	0.5	0.3
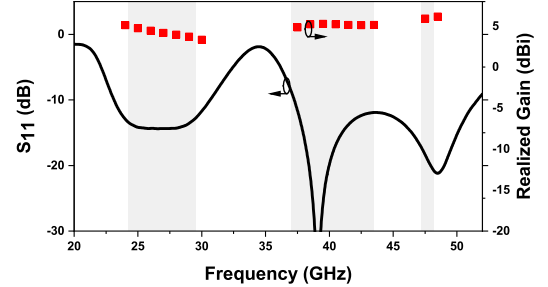
Fig. 2: Simulated reflection coefficient and the realized gain for the antenna element over the operating bands.

Fig. 2 shows the simulated reflection coefficient of the single antenna element. A dual-band operation over the bands (23 - 30 GHz) and (36 - 50 GHz) is achieved in terms of –10 dB impedance matching criterion. In addition, Fig. 2 shows also the simulated realized gain for the single antenna over resonant frequencies of the bands of interest. As can be seen, the antenna element provides a stable gain of at least 3.6 dBi.
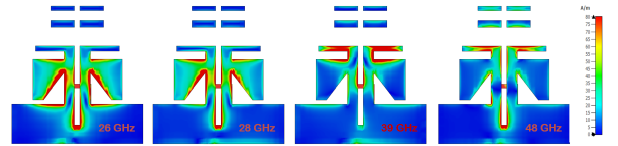
Fig. 3: Simulated current distribution of the single antenna at 26, 28, 39 and 48 GHz.

To further investigate the operating resonances of the antenna, Fig. 3 shows the simulated current distribution for the single antenna at 26 GHz, 28 GHz, 39 GHz and 48 GHz, respectively. As illustrated, most of the currents flow around the bowtie dipole in the lower bands (26 GHz, 28 GHz) whereas, the two protruding strips and the capacitive coupling of parasitic directors with the driven strips are responsible for the higher bands (39 GHz, 48 GHz), respectively.

III. Antenna Array and Simulation Results

The antenna is exemplified based on antenna element with a typical spacing of 28 GHz half-wavelength between the adjacent elements which is approximately 5 mm to ensure a high isolation level, minimize the grating lobes, and achieve a wide beam scanning performance [11]. The antenna module is designed as an array of four elements with overall dimensions of (20 mm x 5.3 mm x 0.127 mm) which can be integrated easily spaced by 2 mm or more from the surrounding metallic

components within the mainboard of a mobile terminal to reduce their effects on the antenna performance to be included in the latest commercial 5G handsets that are capable of tapping the mmWave spectrum.
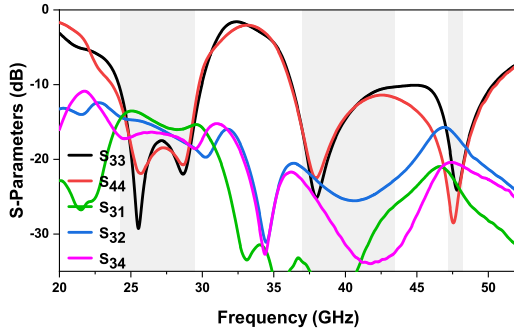
Fig. 4: Simulated S-parameters of the proposed antenna array

Fig. 6 shows the simulated S-parameters of the antenna array. The results indicate that the designed array can entirely cover the frequency bands of interest (24.5-29.5 GHz), (37-43.5 GHz) and (47.2-48.2 GHz). As can be seen, the isolation level is less than 15 dB over the mmWave 5G target bands without any decoupling structures.
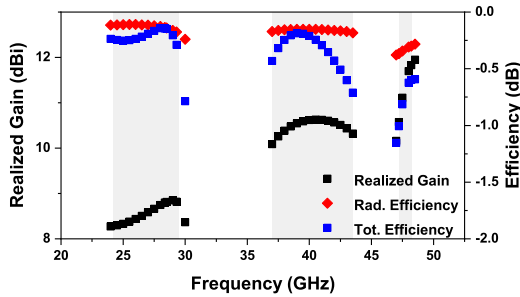
Fig. 5: Simulated realized gain and efficiencies of the array

Fig. 5 depicts the simulated realized gain and efficiencies of the antenna array over the operating bands. As shown, the maximum realized gain ranges from 8.4 dBi to 11.8 dBi, which is sufficient and stable over the 5G NR bands. The array radiation efficiency is higher than -0.36 dB (92%). Besides, the total efficiency is more than -1 dB (80%).

The simulated 3D radiation beam of the proposed antenna array at 0° scanning angle for different frequencies (26, 28, 39, 48 GHz) have been provided in Fig. 6. As can be observed, symmetric and stable endfire radiation patterns with high gain levels have been achieved at different operating bands.

Fig. 7 shows the simulated beam scanning patterns of the proposed 4-elements array antenna throughout $+x$ (+90°) to $-x$ (-90°) (xoy) plane at 26 GHz, 28 GHz, 39 GHz and 48 GHz frequencies, respectively. The array beam scanning has been calculated based on the radiation patterns of each element with equal magnitude and progressive phase shifts between adjacent antennas. From the simulated results of Fig. 7, it can be seen that the beam scanning coverage can
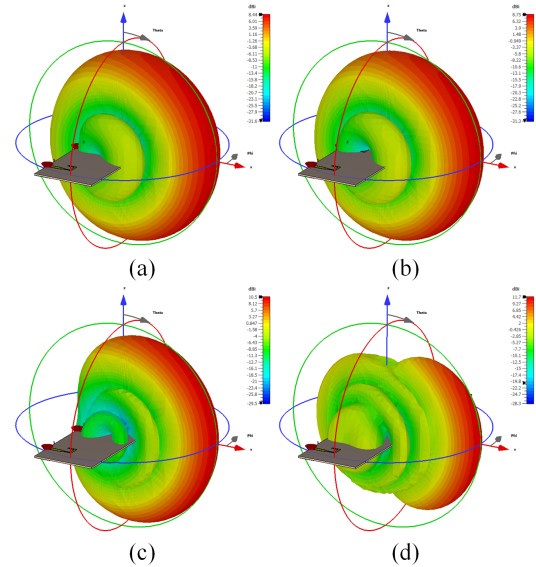
Fig. 6: 3D radiation beams of the antenna array at (a) 26 GHz, (b) 28 GHz, (c) 39 GHz, (d) 48 GHz.

be achieved wherein the minimum required realized gain is defined as -3 dB from the maximum realized gain at 0°. Beam scanning angles are from -72° to +68° at 26 GHz, from -68° to +65° at 28GHz, from -40° to +41° at 39 GHz, and from -33° to +35° at 48 GHz. In the higher frequency bands, the beamwidth is narrower due to the higher array gain. Therefore, compared to the lower bands, the scanning range is limited. Furthermore, the grating lobes are mainly caused by the different inter-element spacings since the wavelength becomes shorter at higher frequencies, which can enlarge the spatial beam coverage.

To further evaluate the merits of the proposed array, the antenna is compared with other recently issued relevant mmWave antenna designs as shown in Table III.

TABLE III: Comparison with Relevant mmWave Endfire Designs

Ref.	[10]	[11]	Proposed Work
Antenna Type	quasi-Yagi	Dipole	quasi-Yagi
Array	1×4	1×8	1×4
Radiation	Endfire	Endfire	Endfire
Operating bands (GHz)	26-40	26.5-38	24.1-29.8 36.2-50
Gain (dBi)	8	10 ∼ 12	8.4 ∼ 11.8
Scanning rang (deg)	±90@28 GHz	±75@28 GHz	-68 ∼ +65@28 GHz -40 ∼ +41@39 GHz -33 ∼ +35@48 GHz

IV. CONCLUSION

A novel tri-band antenna design has been proposed for 5G millimeter-wave applications. The proposed antenna achieves multiband operation to cover 5G NR bands (24.25-29.5 GHz),
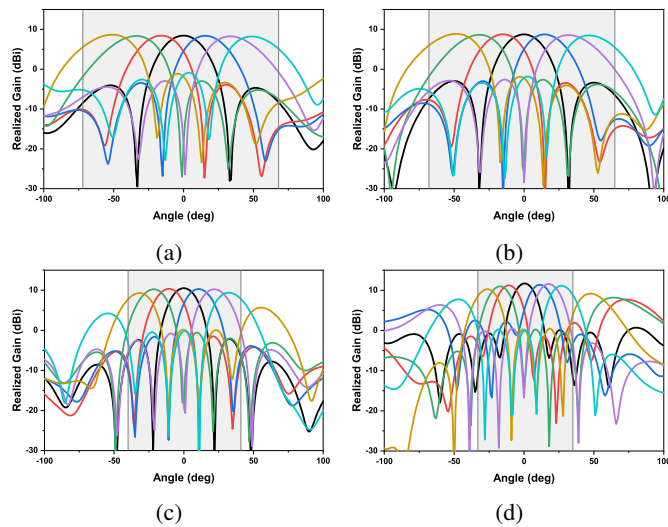
Fig. 7: Simulated beam scanning performance in the horizontal plane (xoy) at (a) 26 GHz, (b) 28 GHz, (c) 39 GHz, (d) 48 GHz.

(37-43.5 GHz), (47.2-48.2 GHz). which is intended for upcoming mmWave mobile communication. The antenna array achieved a maximum gain of 11.8 dBi in the endfire direction and could be utilized as a phased array to steer the radiation beam. The antenna exhibited a very good -3 dB beam scanning pattern and stable gain throughout the bands of interest and can easily be installed within the mobile terminal. The next step is to fabricate the antenna and verify the simulation results.

ACKNOWLEDGMENT

REFERENCES

[1] J. G. Andrews, S. Buzzi, W. Choi, S. V. Hanly, A. Lozano, A. C. Soong, and J. C. Zhang, "What will 5G be?" *IEEE Journal on Selected Areas in Communications*, vol. 32, no. 6, pp. 1065–1082, 2014.

[2] J. Lee, E. Tejedor, K. Ranta-Aho, H. Wang, K. T. Lee, E. Semaan, E. Mohyeldin, J. Song, C. Bergljung, and S. Jung, "Spectrum for 5G: Global Status, Challenges, and Enabling Technologies," *IEEE Communications Magazine*, vol. 56, no. 3, pp. 12–18, 2018.

[3] J. Qiao, X. Shen, J. Mark, Q. Shen, Y. He, and L. Lei, "Enabling device-to-device communications in millimeter-wave 5G cellular networks," *IEEE Communications Magazine*, vol. 53, no. 1, pp. 209–215, 2015.

[4] I. A. Hemadeh, K. Satyanarayana, M. El-Hajjar, and L. Hanzo, "Millimeter-Wave Communications: Physical Channel Models, Design Considerations, Antenna Constructions, and Link-Budget," *IEEE Communications Surveys and Tutorials*, vol. 20, no. 2, pp. 870–913, 2018.

[5] W. Hong, K. H. Baek, Y. Lee, Y. Kim, and S. T. Ko, "Study and prototyping of practically large-scale mmWave antenna systems for 5G cellular devices," *IEEE Communications Magazine*, vol. 52, no. 9, pp. 63–69, 2014.

[6] W. Roh, J.-y. Seol, J. Park, B. Lee, J. Lee, Y. Kim, and J. Cho, "Millimeter-Wave Beamforming as an Enabling Technology for 5G Cellular Communications: Theoretical Feasibility and Prototype Results," *IEEE communications magazine*, vol. 52, no. 2, pp. 106–113, 2014.

[7] J. Helander, K. Zhao, Z. Ying, and D. Sjöberg, "Performance Analysis of Millimeter-Wave Phased Array Antennas in Cellular Handsets," *IEEE Antennas and Wireless Propagation Letters*, vol. 15, no. c, pp. 504–507, 2016.

[8] V. Raghavan, M. L. Chi, M. A. Tassoudji, O. H. Koymen, and J. Li, "Antenna Placement and Performance Tradeoffs with Hand Blockage in Millimeter Wave Systems," *IEEE Transactions on Communications*, vol. 67, no. 4, pp. 3082–3096, 2019.

[9] I. J. Hwang, B. K. Ahn, S. C. Chae, J. W. Yu, and W. W. Lee, "Quasi-Yagi Antenna Array with Modified Folded Dipole Driver for mmWave 5G Cellular Devices," *IEEE Antennas and Wireless Propagation Letters*, vol. 18, no. 5, pp. 971–975, 2019.

[10] C. Di Paola, S. Zhang, K. Zhao, Z. Ying, T. Bolin, and G. F. Pedersen, "Wideband Beam-Switchable 28 GHz Quasi-Yagi Array for Mobile Devices," *IEEE Transactions on Antennas and Propagation*, vol. 67, no. 11, pp. 6870–6882, 2019.

[11] S. X. Ta, H. Choo, and I. Park, "Broadband Printed-Dipole Antenna and Its Arrays for 5G Applications," *IEEE Antennas and Wireless Propagation Letters*, vol. 16, no. c, pp. 2183–2186, 2017.

[12] S. Zhu, H. Liu, Z. Chen, and P. Wen, "A compact gain-enhanced vivaldi antenna array with suppressed mutual coupling for 5G mmwave application," *IEEE Antennas and Wireless Propagation Letters*, vol. 17, no. 5, pp. 776–779, 2018.

[13] T. Li and Z. N. Chen, "Wideband Substrate-Integrated Waveguide-Fed Endfire Metasurface Antenna Array," *IEEE Transactions on Antennas and Propagation*, vol. 66, no. 12, pp. 7032–7040, 2018.

[14] T. Specification, "Ts 138 508-2 - V17.4.0 - TECHNICAL SPECIFICATION 5G; LTE; 5GS; User Equipment (UE) conformance specification; Part 2: Common Implementation Conformance Statement (ICS) proforma," vol. 18, 2022.

[15] W.-y. Li, W. Chung, and K.-l. Wong, "Highly-Integrated Dual-Band mmWave Antenna Array for 5G Mobile Phone Application," in *2020 14th European Conference on Antennas and Propagation (EuCAP)*, 2020, pp. 1–5.

[16] T. Li and Z. N. Chen, "A dual-band metasurface antenna using characteristic mode analysis," *IEEE Transactions on Antennas and Propagation*, vol. 66, no. 10, pp. 5620–5624, 2018.

[17] M. Stanley, Y. Huang, H. Wang, H. Zhou, A. Alieldin, S. Joseph, C. Song, and T. Jia, "A Dual-Band Dual-Polarised Stacked Patch Antenna for 28 GHz and 39 GHz 5G Millimetre-Wave Communication," *13th European Conference on Antennas and Propagation, EuCAP 2019*, no. EuCAP, pp. 1–4, 2019.

[18] Y. He, S. Lv, L. Zhao, G. L. Huang, X. Chen, and W. Lin, "A Compact Dual-Band and Dual-Polarized Millimeter-Wave Beam Scanning Antenna Array for 5G Mobile Terminals," *IEEE Access*, vol. 9, pp. 109 042–109 052, 2021.